



Cite this: *Chem. Commun.*, 2015, 51, 847

Received 28th October 2014,  
Accepted 21st November 2014

DOI: 10.1039/c4cc08513b

www.rsc.org/chemcomm

## A photoswitchable supramolecular complex with release-and-report capabilities†

Jesper R. Nilsson,<sup>a</sup> Melanie C. O'Sullivan,<sup>b</sup> S. Li,<sup>a</sup> Harry L. Anderson<sup>b</sup> and Joakim Andréasson<sup>\*a</sup>

**A self-assembled supramolecular platform has been designed for reversibly controlling the concentration of a compound in solution, via a photochemical reaction. The system utilizes metal–ligand interactions between a Zn-porphyrin dimer and a pyridine-appended dithienylethene (DTE) photoswitch. In addition to reversible compound release, the spectral properties of the release scaffold provide a fluorescence-based reporting function.**

Controlling when and where a substance is released and/or captured has great potential in a wide range of applications, *e.g.* the release of therapeutic compounds, sensing agents, or extraction of hazardous chemicals and pollutants. The unique properties of light sets it aside as a triggering stimulus for applications requiring spatiotemporally well-resolved, waste-free operation.<sup>1</sup> A number of approaches have been investigated in pursuit of light-operated release systems and these efforts have consequently stimulated a rapidly progressing and inventive research field. A majority of the so far reported light-controlled release systems, however, are designed to exhibit irreversible release. This is typically achieved by light-induced cleavage of covalent bonds either directly using photolabile groups/linkers<sup>2</sup> or second-hand by first generating for instance heat.<sup>3</sup> Another well explored approach is the preparation of light-responsive drug loaded materials such as porous materials<sup>4</sup> and/or micro/nanoparticles.<sup>5</sup>

An additional level of control is attained if the photo-release can be made reversible, as it allows for dynamic bidirectional control of the concentration profile in combination with precise timing of the dosage. Realization of such systems typically demands a photoswitchable component capable of interacting non-covalently with a host compound to form a supramolecular complex. There are

several examples where this concept has been successfully implemented to manipulate for instance the release of small ions,<sup>6</sup> as well as small molecules<sup>7</sup> in a reversible manner. A particularly elegant example of photoreversible compound release was reported in the recent work by Clever and co-workers in which a photoswitchable coordination cage composed of Pd-coordinating dithienylethenes (DTEs) was shown to reversibly encapsulate inorganic guest molecules in response to light.<sup>7b</sup>

In this work, we report a conceptually different coordination-based approach for compound (capture and) release. Here, the differences in binding mode and binding strength between the two isomeric forms of a pyridine-appended DTE photoswitch (**1**, see Fig. 1) and a porphyrin dimer (**P<sub>2</sub>**) are combined into a self-assembled platform with release-and-report capabilities for lone pair-carrying guest molecules.

Since its discovery, the DTE-backbone has found regular use in photoswitching applications due to its renowned high degree of photoconversion, thermal stability, and resistance to photofatigue.<sup>8</sup> The photoinduced ring-closing (**1o** → **1c**) is achieved with 302 nm UV-light ( $\Phi_{o \rightarrow c} = 0.57$ )<sup>9</sup> and converts the sample to virtually 100% **1c**. Subsequent visible light exposure ( $\lambda > 550$  nm) completely opens the sample to **1o** ( $\Phi_{c \rightarrow o} = 0.02$ ). This switching cycle can be repeated several times without notable photodegradation<sup>10</sup> (see Fig. S3 for absorption spectra of **1**, and ESI† for details on isomerization quantum yield).

Porphyrin macrocycles have been included in numerous molecular and supramolecular constructs as building blocks with fluorescent, sensitizing, and/or energy/electron transfer capabilities.<sup>11</sup> The two porphyrin units constituting the herein used **P<sub>2</sub>** have a near-barrierless rotation around the central diethyne axis, thus allowing an even distribution of rotamers in the dimer.<sup>12</sup> The aliphatic side chains (Ar and R in Fig. 1) effectively prevent dimer stacking, as no aggregation was detected up to mM concentrations. As for coordination to **P<sub>2</sub>**, the two DTE-isomers **1o** and **1c** are notably different. The ring-closed isomer (**1c**) coordinates axially to one Zn-center in **P<sub>2</sub>** by donating a pyridine electron lone pair. This complexation occurs in a consecutive 1:1 → 1:2 manner, with binding

<sup>a</sup> Department of Chemical and Biological Engineering, Chalmers University of Technology, SE-412 96 Göteborg, Sweden. E-mail: a-son@chalmers.se; Fax: +46-31-772-3858; Tel: +46-31-772-2838

<sup>b</sup> Department of Chemistry, Oxford University, Oxford OX1 3TA, UK. E-mail: harry.anderson@chem.ox.ac.uk; Fax: +44-(0)1865-2-85002; Tel: +44-(0)1865-2-75704

† Electronic supplementary information (ESI) available: Synthetic procedure for **G-Pe**, spectroscopic details. See DOI: 10.1039/c4cc08513b



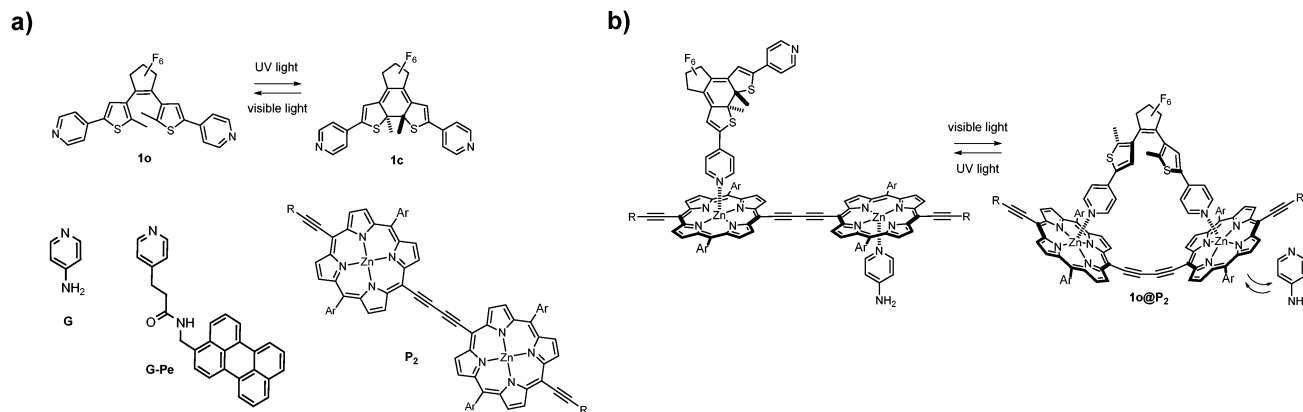


Fig. 1 (a) Isomerization scheme of **1** and molecular structures of 4-aminopyridine (**G**), the perylene functionalized analog (**G-Pe**), and the porphyrin dimer (**P2**). (b) Photo-release principle. Ar = Si(C<sub>6</sub>H<sub>13</sub>)<sub>3</sub>, R = 3,5-di(*tert*-butyl)phenyl.

constants of  $K_{a1} = 6.1 \times 10^5 \text{ M}^{-1}$  and  $K_{a2} = 6.0 \times 10^4 \text{ M}^{-1}$ , respectively as determined by UV/Vis titrations (see ESI† for titration details). For non-cooperative binding to a two-site host;  $K_{a1} = 4 \times K_{a2}$ , indicating that binding of the second **1c** to **P2** exhibits slightly negative cooperativity, possibly due to minor steric interactions. In sharp contrast, the structural flexibility of the ring-opened isomer (**1o**) allows it to stretch and instead form a 1:1 staple-like complex (**1o@P2**, Fig. 1). As a result of the double axial Zn-coordination, the latter binding is significantly stronger ( $K_a = 5.5 \times 10^6 \text{ M}^{-1}$ ), in effect causing initially bound compounds to be released into solution as a result of competitive binding. The **1o@P2** 1:1 binding stoichiometry is strongly supported by the existence of no less than 8 isosbestic points throughout the **1o** to **P2** titration (Fig. S4, ESI†). There is also a clear resemblance to the spectral changes seen upon **P2** planarization using static (non-photochromic) ligands.<sup>12</sup> Furthermore, the **1o@P2** binding mode has been assessed by computational means.<sup>10</sup> Binding of **1** to **P2** has no significant effect on the rate of the photoinduced ring-opening reaction, while the corresponding closing rate is reduced by a factor of 6. This is likely due to coordination-induced restrictions in the conformational flexibility required for the isomerization process to occur. The usefulness of combining photoswitchable units and metalloporphyrins/porphyrinoids in supramolecular strategies is evidenced by the wide variety of processes brought under reversible photonic control using these building blocks. These include emission intensity,<sup>13</sup> energy transfer,<sup>14</sup> electron transfer,<sup>15</sup> magnetic properties,<sup>16</sup> and singlet oxygen generation.<sup>17</sup>

Here, the drug chosen to illustrate the release event is the well known small molecule neurotransmitter 4-aminopyridine (**G**, see Fig. 1).<sup>18</sup> In principle, any monodentate Lewis base can be used, the main prerequisite being adequate coordination capabilities (*i.e.* suitable binding strength) to Zn in **P2**. However, any change in the UV/Vis absorption of **G** upon coordination to **P2** is obscured by the corresponding changes of the latter. Hence, a more straightforward means of monitoring binding/release of **G** is needed. Therefore, **G-Pe** was synthesized as a fluorescent model compound. **G** and **G-Pe** have identical binding modes to **P2**. The binding constants are:  $K_{a1} = 3.2 \times 10^5 \text{ M}^{-1}$ ,  $K_{a2} = 1.2 \times 10^5 \text{ M}^{-1}$  and  $K_{a1} = 1.3 \times 10^5 \text{ M}^{-1}$ ,  $K_{a2} = 3.6 \times 10^4 \text{ M}^{-1}$  for **G** and **G-Pe** respectively. The choice of the

peryene fluorophore is motivated by the excellent spectral overlap between the emission spectra of **G-Pe**, and the **P2** Soret band. Hence, binding to **P2** efficiently quenches the **G-Pe** emission by excitation energy transfer (EET,  $R_0 = 66 \text{ Å}$ , see Fig. S12 for details, ESI†), possibly in combination with electron transfer (ET). Accordingly, the observed **G-Pe** emission originates exclusively from compound free in solution. It should be noted that **G-Pe** has nothing to do with the function of the release scaffold *per se*; it is used merely as a tool for monitoring the release.

The release of **G-Pe** is demonstrated in Fig. 2, where an initial cocktail of **P2**, **1o**, and **G-Pe** gives rise to high emission, as the strongly coordinating **1o** occupies both Zn binding-sites in **P2**. Subjecting the solution to UV-light causes a **1o** → **1c** isomerization, whereafter each DTE-unit cannot coordinate more than one Zn-center. In response, **G-Pe** binds to the liberated coordination site,

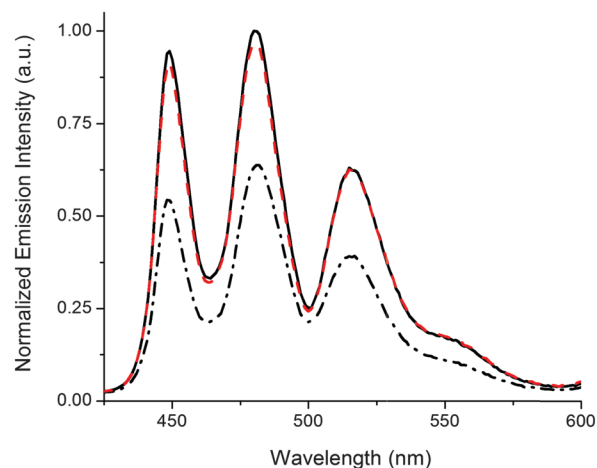


Fig. 2 Reversible release of **G-Pe** in response to light monitored by the emission intensity of the uncomplexed **G-Pe** population. Applied concentrations; [**P2**] = 280  $\mu\text{M}$ , [**1**] = 300  $\mu\text{M}$ , [**G-Pe**] = 1  $\mu\text{M}$ . Initially, **1** is in the open form **1o** (solid black line). 2 min 302 nm UV-exposure triggers isomerization to **1c** (dash-dotted black line). Subsequent visible light isomerizes the sample back to **1o** ( $\lambda > 550 \text{ nm}$ , 3 min, dashed red line). Please note that the experimental conditions/setup allows emission intensities unaffected by isomerization-induced inner filter effects.‡



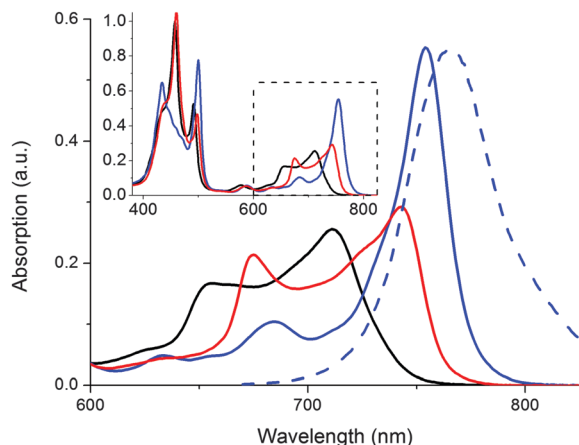


Fig. 3 Absorption spectra of supramolecular  $P_2$ -complexes in toluene:  $P_2$  (black line),  $2G@P_2$  (red line), and the planarized  $1o@P_2$  (blue line). The blue dashed line shows the  $1o@P_2$  emission spectra ( $\lambda_{exc} = 510$  nm). Inset: Absorption from 380–825 nm.

and the emission is quenched. Subsequent visible light restores the high emission by reforming  $1o$  and displacement of  $G-Pe$  from  $P_2$ .

In addition to triggering the compound release, formation of the doubly coordinated  $1o@P_2$  complex forces the two porphyrin macrocycles to adopt a coplanar conformation. With this restriction in  $P_2$  rotameric distribution comes characteristic changes in the absorption spectrum (Fig. 3).

In Fig. 3, the absorption spectral signatures of  $P_2$  and the two types of  $P_2$  complexes are shown. Monodentate species typically induce a red-shift in the  $P_2$  Q-band ( $711$  nm  $\rightarrow$   $\sim 745$  nm). The planar complex ( $1o@P_2$ ) exhibits a further red shifted, and significantly hyperchromic absorption band centered at  $754$  nm. The spectral features inherent to the rotational distribution of diethyne-linked porphyrin dimers and oligomers have been used to control the rate of electron transfer<sup>19</sup> as well as singlet oxygen generation,<sup>20</sup> by allowing selective excitation of planar or randomly oriented rotamers. In our laboratory, we have devised a molecular memory capable of non-destructive readout based on photochromic planarization of a porphyrin dimer.<sup>10</sup> Here, as the compound release proceeds concurrently with a marked increase in absorption of  $P_2$  around  $750$  nm, it is possible to read the state of the release scaffold to confirm the release event by probing the emission at  $800$  nm, following excitation at  $790$  nm. Hence, the inherent fluorescent properties of the scaffold are in line with the so-called release-and-report function.

The typical “release” (e.g. caged compounds<sup>2b</sup>) requires UV-light. For most light-controlled applications, this is not optimal, due to limited penetration depth and potential damage to surrounding tissue, materials, and/or the released compound itself. Here, a notable advantage is that both the release- and the report functions are triggered by low energy photons ( $\lambda$  up to ca.  $700$  nm and almost  $800$  nm, respectively). To illustrate the performance and stability of the release scaffold, we prepared a sample containing  $P_2$ ,  $1o$ , and  $G$ , and subjected the solution to alternating irradiation of  $302$  nm and visible light ( $\lambda > 550$  nm), probing the report output after each irradiation step (Fig. 4).

It is clear that  $1c \rightleftharpoons 1o$  isomerization causes dramatic differences in emission intensity from  $P_2$ , and that switching

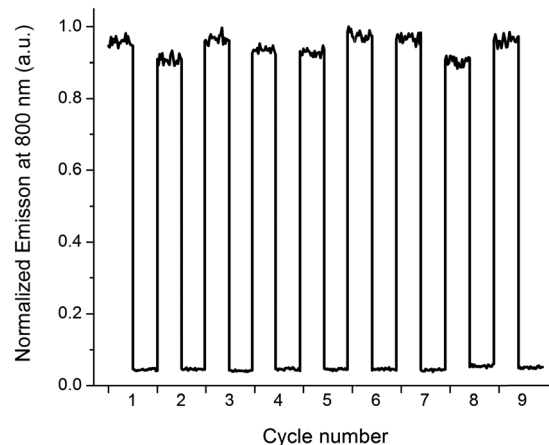


Fig. 4 Photoswitching performance of the release-and-report system, as monitored via the report function, i.e. emission intensity at  $800$  nm ( $\lambda_{exc} = 790$  nm). Applied concentrations;  $[P_2] = 280$   $\mu$ M,  $[1] = 300$   $\mu$ M,  $[G] = 1$   $\mu$ M. Each cycle starts with  $1$  in the open form  $1o$  (high intensity).  $2$  min  $302$  nm UV-exposure triggers isomerization to  $1c$  (low intensity). Subsequent visible light ( $\lambda > 550$  nm,  $3$  min) isomerizes the sample back to  $1o$ .

between the two types of complexes is fully reversible, and proceeds with no apparent photodegradation.

The authors appreciate the limited biological compatibility of the solvents used throughout this proof-of-principle study. Thus, for use in biological environments, solubilization of the release scaffold needs to be addressed. In this context it deserves mentioning that metal-ligand coordination approaches to photo-release (albeit irreversible) in living organisms have been reported,<sup>21</sup> along with examples of porphyrin dimers<sup>22</sup> and DTEs<sup>23</sup> adapted for, and used in, biological applications.

A self-assembled system for reversible photo-control of compound release has been demonstrated. The unique spectral properties inherent to this system conveniently allows for fluorescence-based assessment of the state of the release scaffold, i.e. whether the compound is bound or not. This reporter ability has to our knowledge not been demonstrated in a reversible release system to date; thus this work represents a conceptually valuable addition to existing photo-operated release systems. The affinity of Zn-porphyrins for amine-based ligands implies that this reversible release system could be applied to a wide range of ligands, eliminating the need for guest-specific synthetic efforts.

This work was financed by the Swedish Research Council (Grant 622-2010-280) and the European Research Council (ERC FP7/2007–2013 Grant No. 203952). Professor Neil Branda is acknowledged for valuable discussions.

## Notes and references

‡ Under the selected conditions,  $[1]$  and  $[P_2]$  give rise to a significant optical density in the solution. It should therefore be noted that the emission measurements were performed in a  $1$  mm cuvette with front-face detection and excitation at an isosbestic point,  $\lambda_{exc} = 410$  nm.

- 1 R. Göstl, A. Senf and S. Hecht, *Chem. Soc. Rev.*, 2014, **43**, 1982.
- 2 (a) K. L. Ciesinski and K. J. Franz, *Angew. Chem., Int. Ed.*, 2011, **50**, 814; (b) C. Brieke, F. Rohrbach, A. Gottschalk, G. Mayer and A. Heckel, *Angew. Chem., Int. Ed.*, 2012, **51**, 8446; (c) P. Klán,



- T. Šolomek, C. G. Bochet, A. Blanc, R. Givens, M. Rubina, V. Popik, A. Kostikov and J. Wirz, *Chem. Rev.*, 2012, **113**, 119; (d) C. G. Bochet, *J. Chem. Soc., Perkin Trans. 1*, 2002, 125.
- 3 (a) A. B. S. Bakhtiari, D. Hsiao, G. Jin, B. D. Gates and N. R. Branda, *Angew. Chem., Int. Ed.*, 2009, **48**, 4166; (b) W. F. Zandberg, A. B. S. Bakhtiari, Z. Erno, D. Hsiao, B. D. Gates, T. Claydon and N. R. Branda, *J. Nanomed. Nanotechnol.*, 2012, **8**, 908.
- 4 (a) N. K. Mal, M. Fujiwara, Y. Tanaka, T. Taguchi and M. Matsukata, *Chem. Mater.*, 2003, **15**, 3385; (b) E. Aznar, M. D. Marcos, R. Martínez-Mañez, F. Sancenón, J. Soto, P. Amorós and C. Guillem, *J. Am. Chem. Soc.*, 2009, **131**, 6833; (c) J. Lu, E. Choi, F. Tamanoi and J. I. Zink, *Small*, 2008, **4**, 421; (d) R. Tong, H. D. Hemmati, R. Langer and D. S. Kohane, *J. Am. Chem. Soc.*, 2012, **134**, 8848.
- 5 (a) H. Yan, C. Teh, S. Sreejith, L. Zhu, A. Kwok, W. Fang, X. Ma, K. T. Nguyen, V. Korzh and Y. Zhao, *Angew. Chem., Int. Ed.*, 2012, **51**, 8373; (b) M. S. Yavuz, Y. Cheng, J. Chen, C. M. Copley, Q. Zhang, M. Rycenga, J. Xie, C. Kim, K. H. Song, A. G. Schwartz, L. V. Wang and Y. Xia, *Nat. Mater.*, 2009, **8**, 935; (c) W. Xiao, W.-H. Chen, J. Zhang, C. Li, R.-X. Zhuo and X.-Z. Zhang, *J. Phys. Chem. B*, 2011, **115**, 13796.
- 6 (a) M. Blank, L. Soo, H. Wassermann and B. Erlanger, *Science*, 1981, **214**, 70; (b) S. Lee and A. H. Flood, *J. Phys. Org. Chem.*, 2013, **26**, 79.
- 7 (a) H. Dube and J. Rebek, *Angew. Chem., Int. Ed.*, 2012, **51**, 3207; (b) M. Han, R. Michel, B. He, Y.-S. Chen, D. Stalke, M. John and G. H. Clever, *Angew. Chem., Int. Ed.*, 2013, **52**, 1319; (c) Y. Wang, M. Zhang, C. Moers, S. Chen, H. Xu, Z. Wang, X. Zhang and Z. Li, *Polymer*, 2009, **50**, 4821; (d) G. H. Clever, S. Tashiro and M. Shionoya, *J. Am. Chem. Soc.*, 2010, **132**, 9973.
- 8 M. Irie, *Chem. Rev.*, 2000, **100**, 1685.
- 9 Quantum yield for the ring-closing reaction was determined in methanol in; K. Matsuda, Y. Shinkai, T. Yamaguchi, K. Nomiya, M. Isayama and M. Irie, *Chem. Lett.*, 2003, **32**, 1178.
- 10 J. Kärrbratt, M. Hammarson, S. Li, H. L. Anderson, B. Albinsson and J. Andréasson, *Angew. Chem., Int. Ed.*, 2010, **49**, 1854.
- 11 (a) I. Beletskaya, V. S. Tyurin, A. Y. Tsivadze, R. Guillard and C. Stern, *Chem. Rev.*, 2009, **109**, 1659; (b) C. A. Hunter and R. K. Hyde, *Angew. Chem., Int. Ed.*, 1996, **35**, 1936.
- 12 M. U. Winters, J. Kärrbratt, M. Eng, C. J. Wilson, H. L. Anderson and B. Albinsson, *J. Phys. Chem. C*, 2007, **111**, 7192.
- 13 (a) T. B. Norsten and N. R. Branda, *Adv. Mater.*, 2001, **13**, 347; (b) J. Otsuki and K. Narutaki, *Bull. Chem. Soc. Jpn.*, 2004, **77**, 1537; (c) D. R. Reddy and B. G. Maiya, *Chem. Commun.*, 2001, 117.
- 14 J. Otsuki, A. Yasuda and T. Takido, *Chem. Commun.*, 2003, 608.
- 15 A. J. Myles and N. R. Branda, *J. Am. Chem. Soc.*, 2000, **123**, 177.
- 16 S. Thies, H. Sell, C. Bornholdt, C. Schütt, F. Köhler, F. Tucek and R. Herges, *Chem. – Eur. J.*, 2012, **18**, 16358.
- 17 L. Hou, X. Zhang, T. C. Pijper, W. R. Browne and B. L. Feringa, *J. Am. Chem. Soc.*, 2014, **136**, 910.
- 18 M. Müller, P. W. Dierkes and W.-R. Schlue, *Brain Res.*, 1999, **826**, 63.
- 19 M. U. Winters, J. Kärrbratt, H. E. Blades, C. J. Wilson, M. J. Frampton, H. L. Anderson and B. Albinsson, *Chem. – Eur. J.*, 2007, **13**, 7385.
- 20 M. K. Kuimova, M. Balaz, H. L. Anderson and P. R. Ogilby, *J. Am. Chem. Soc.*, 2009, **131**, 7948.
- 21 L. Zayat, C. Calero, P. Alborés, L. Baraldo and R. Etchenique, *J. Am. Chem. Soc.*, 2003, **125**, 882.
- 22 M. K. Kuimova, S. W. Botchway, A. W. Parker, M. Balaz, H. A. Collins, H. L. Anderson, K. Suhling and P. R. Ogilby, *Nat. Chem.*, 2009, **1**, 69.
- 23 T. C. S. Pace, V. Müller, S. Li, P. Lincoln and J. Andréasson, *Angew. Chem., Int. Ed.*, 2013, **52**, 4393.

